Development of integrated roof monitoring system and continuous miner working index for improving mine safety

Banda Srikanth*

Department of ECE,
University College of Engineering,
Kakatiya University,
Kothagudem, Telangana, 507101, India
Email: bsrikanthiitkgp@gmail.com
*Corresponding author

Hemant Kumar

Department of Mining Engineering,
Indian Institute of Technology (ISM),
Dhanbad, Jharkhand, 826004, India
Email: hemant@iitism.ac.in

Srinivasulu Tadisetty

Department of ECE,
Kakatiya University,
Warangal, Telangana, 506009, India
Email: drstadisetty@gmail.com

Abstract: Roof falls are the major catastrophes that occur in the underground coal mines and these falls have a serious impact on workmen in terms of injuries, fatality, and interruptions of production. Hence continuous monitoring of roof convergence is important to predict roof fall. A suitable monitoring system for roof convergence may be installed in underground mines to mitigate problems associated with roof falls. This paper explains the development of a new real-time integrated roof monitoring system based on an ultrasonic distance measurement sensor that has been deployed in the continuous miner workings for the measurement of roof convergence. The roof convergence data is processed to develop the continuous miner working index (CMWI) using statistical techniques and CMWI is very useful for predicting roof convergence in continuous miner workings to improve the safety of operations.

Keywords: roof fall; roof convergence; ultrasonic-based monitoring system; mine index; continuous miner working index; CMWI.

Reference to this paper should be made as follows: Srikanth, B., Kumar, H. and Tadisetty, S. (2022) 'Development of integrated roof monitoring system and continuous miner working index for improving mine safety', *Int. J. Mining and Mineral Engineering*, Vol. 13, No. 1, pp.1–17.

Biographical notes: Banda Srikanth received his MTech degree in Microelectronics and VLSI Design from the Department of Electronics and Communication Engineering, IIT Kharagpur, India in 2008. He is currently an Assistant Professor at the University College of Engineering (KU), Bardradri Kothagudem, Telangana, India. He is pursuing his PhD in Mining Engineering from IIT(ISM) Dhanbad. His current research interest includes embedded system application in underground coal mines, IOT and machine learning.

Hemant Kumar received his PhD degree from the Department of Mining Engineering at IIT Kharagpur, Kharagpur, India in 2013. He is currently an Assistant Professor in the Department of Mining Engineering, IIT(ISM) Dhanbad, Jharkhand, India. His research interest includes rock mechanics, underground metal mining, mine ventilation and mine safety.

Srinivasulu Tadisetty received his PhD degree from the Department of Electronics and Communication Engineering Faculty of Engineering Technology, Japan, Kyushu University in 2005. He is currently a Professor at the Department of Electronics and Communication Engineering, Warangal, Telangana, India. His research interest includes embedded system application in underground coal mines, IOT, WSN, 5G communications and machine learning.

1 Introduction

Roof falls constitute a major category of natural calamity in underground coal mines and major roof falls may cause injury, death, and delay in production. Roof falls threaten workers, damage machinery, obstruct the ventilation airways, and emergency escape routes. It is very difficult to protect mine workers unless the roof and sides are monitored and controlled meticulously. Strata monitoring and control methods are the key techniques for creating a safe environment and improving the performance of mine in terms of safety and productivity.

Mining organisations, research, academic institutes, and mining statutory bodies (DGMS) of India have been making continuous efforts to mitigate accidents in Indian mines and have imposed legislative rules, imparting training, introducing various technologies in roof monitoring, and at the cutting face. The occurrence of fatal accidents in Indian underground coal mines is more than that of the USA, Australia, and other western countries (DGMS, 2017; MSHA, 2017). It is also observed from studies that there is a decreasing pattern in the number of fatal Incidents per lakh man shifts, death rates per 1,000 workers, and death rates per million tons in Indian coal mines. However, existing statistical evidence of fatalities is still cause for concern.

The roof falls contribute to the occurrence of most fatal accidents in the underground mine. To mitigate roof fall hazards in mines, an automated integrated real-time roof fall warning monitoring system is needed to withdraw miners before the occurrence of roof falls. Further, it is also necessary to develop a unified index by combining all the geo-mining parameters to estimate the convergence developed in the continuous miner workings.

Extensive research studies have been published on various roof monitoring integrated systems to monitor the convergence, and load in underground coal mines. For instance, Swanson (2002) examined roof fall hazards in underground coal mines using a

non-contact laser-based vibration measurement. Shen et al. (2008) investigated roof stability of tailgate roadways due to an increase in vertical stress in underground coal mines of Australia. Atul et al. (2010) developed an intrinsically safe system and installed it at longwall face to continuously monitor load and convergence of powered roof supports. Kumarghosh et al. (2011) found a roof fall precursor to predicting roof fall in underground mines. Zhao et al. (2015) used fibre Bragg grating (FBG) displacement sensor to monitor roof separation in coal mine roadways. Buddery et al. (2018) investigated standing support density and capacity at various locations throughout the tailgate based on roof convergence (RC) data generated by Integrated monitoring system. Zhang et al. (2018) used inertial MEMS type sensors to examine cracks and displacement characteristics of strata in coal mines. Indra et al. (2018) developed a prototype-based electromechanical tell-tale system that uses electronic and mechanical components such as sensors and spring - pulley system. This system gives visual roof fall warnings to miners. Jena et al. (2019) established a conceptual model for roof fall warning index. Gong et al. (2019) pointed out the unique feature and major differences between traditional geotechnical control instruments and fibber optic sensing (FOS).

Verma and Deb (2010) derived the face stability parameters of longwall to estimate shield load and convergence. Katkuri et al. (2020) conducted a study to know the stability of the gate roadways based on field data and the application of the ANN technique. Islavath et al. (2020) developed convergence index to predict the longwall face convergence.

In this study, the authors have developed an integrated monitoring system that includes ultrasonic displacement, temperature, and humidity sensors. The integrated system uses a micro-SD card module to record data of RC. This research focuses on the design and evaluation of real-time continuous monitoring of RC using an integrated real-time monitoring system, which includes a MEMS type ultrasonic displacement sensor that does not require any wire connection from roof to the floor to measure convergence. Data transmission from the monitoring station to a destination (safe zone in the underground) is transferred using Wireless data transceivers. This system is deployed in VK7 mine of Kothagudem, Singareni Collieries Company Limited, Telangana. The RC data was recorded using the developed system and this data was compared with the tell-tale data and was found to be more or less the same. The RC data of three continuous miner panels were collected and the convergence data was further processed for the development of a continuous miner working index (CMWI) to predict the RC of future continuous miner panels.

2 Development of ultrasonic-based continuous roof convergence monitoring system

The ultrasonic-based continuous roof convergence monitoring system (U-CRCMS) consists of two major parts, these being the transmitter and receiver. This system was deployed in the continuous miner panel and records the RC. The RC values are sent to the receiver through wireless. The receiver was kept in a safe zone in an underground mine. A detailed description of the system is given below.

2.1 Transmitter section

The transmitter section consists of five major modules, namely ultrasonic displacement sensor, temperature sensor, micro-SD card adapter, Real-time clock, and a wireless transceiver, and all of them are interconnected with a microcontroller called real-time integrated monitoring system (transmitter section), as shown in Figure 1. The system has been deployed in the roof of continuous miner workings. The sensors are interconnected directly to the microcontroller because all peripheral devices are compatible with a microcontroller. Both the transmitter and receiver units are intrinsically safe to function without any possibility of damage in an environment that experiences high temperature and humidity.

Figure 1 Transmitter section

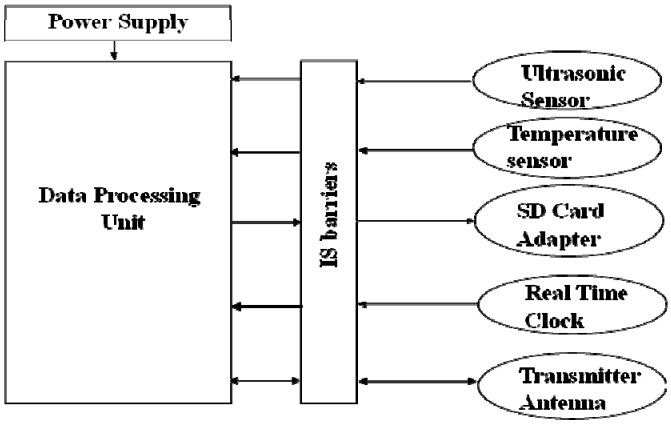

2.1.1 Ultrasonic displacement sensor

The convergence monitoring system employs the ultrasonic displacement sensor. It is a low-cost device consisting of a transmitter module that emits ultrasonic pulses and a receiver module that receives the reflected ultrasonic pulses after hitting any solid objects. An ultrasonic sensor delivers a pulse to the target and receives reflecting signals from the surface, as shown in Figure 2 (Panda et al., 2016).

The main function of the data acquisition system (DAS) is to send a high pulse length of 10 μs to the ultrasonic sensor. In response to the DAS pulse, the ultrasonic sensor transmits a series of 8 clock pulses with a 40 KHz frequency. When an object exists beyond the range of sensor limitation, the sensor receives an echo pulse. In response to the received echo, the ultrasonic sensor produces an equal distance high pulse through the ECHO pin and sends it to the DAS. For ultrasonic sensor operation with a range of centimetres, if DAS takes a fixed sound speed, the output error is acceptable to some extent. But the error due to fixed sound speed would not be appropriate in the case of operations with a millimetre range. DAS, therefore, requires instantaneous speed of sound instead of the fixed speed for the operation of a millimetre. This sensor is compatible with a microcontroller and therefore no level converter is needed. The technical specifications of the ultrasonic displacement sensor are as follows:

1 distance measurement range 2 cm to 4 m

2 accuracy: 1 mm

3 operating frequency: 40 KHz.

Figure 2 Working principle of ultrasonic sensor (see online version for colours)

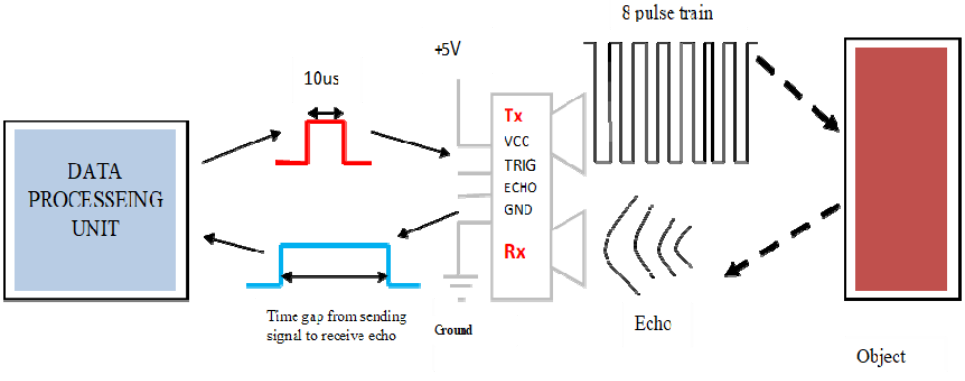

2.1.2 Transmitter antenna

A transmitter antenna is an embedded radio transceiver. The transceiver is an integration of frequency synthesiser, power amplifier, demodulator, modulator, crystal oscillator, and protocol engine. Output control, frequency channels, and protocol configuration can be easily programmable via a serial peripheral interface (SPI). In receiver mode, current consumption is very low, with a peak current of just 9.0 mA. The combined shut down and standby modes enable power savings and are simple to achieve. Some salient features of the transceiver are as follows:

1 global 2.4 GHz ISM band

2 speed 250 kbps, 1 Mbps, and 2 Mbps

3 ultra-low power.

2.1.3 SD card adapter

The micro-SD card module is used for a data logging purposes. The microcontroller uses the SD library to create a file in an SD card to write and save data. There are different models from different suppliers, but they all work similarly, using the SPI communication protocol.

2.1.4 Temperature and humidity sensor

The temperature and humidity sensor is used to measure temperature and humidity in underground coal mines. The purpose of using the sensor in the system is that, the distance measured by ultrasonic sensor varies with the speed of sound which depends upon temperature and humidity (Nicolau et al., 2009). The sensor can measure

temperature and humidity ranging from –40°C to +125°C with ± 0.5 degrees accuracy and from 0 to 100% with 2 to 5% accuracy.

2.1.5 Real-time clock

A real-time clock is used for measuring time while obtaining roof-to-floor convergence data after deploying the integrated monitoring system in the underground coal mine for field study. The device has separate battery backup facility to get real-time measurements at the time of field study.

2.2 Receiver section

The receiver unit consists of one microcontroller, one display, a micro-SD card adapter, display, and receiver antenna. This unit collects the RC data sent from the wireless transmitter unit. The data are then analysed and displayed automatically in real-time on a mine site at the receiver section. Figure 3 shows the block diagram of the receiver; this unit is located in a non-hazardous and serviced location in an underground mine.

Figure 3 Receiver section

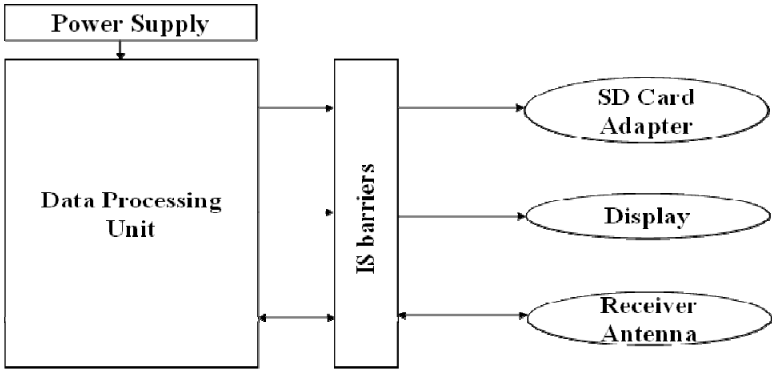

2.2.1 Display unit

The display unit is used to monitor convergence data physically. The display unit is a single-chip CMOS OLED driver controller. It can interact in several ways with microcontrollers like inter-integrated circuit (I2C) and SPI protocols. SPI protocol communication is normally faster than I2C communication but needs more input/output pins (I / O pins). I2C needs only two I/O pins and the pins can be used by other peripheral I2C devices.

The operation of the receiver antenna is the same as that of the transceiver, as discussed in the transmitter section. The operation of the micro-SD card is also addressed in the transmitter section.

3 Field study

The developed Integrated real-time monitoring system deployed in the continuous miner panel of VK 7 mine, Kothagudem area, SCCL. The details of the case study mine and procedure adopted for roof monitoring are given below.

3.1 Mine description

The mine consists of three seams namely top, king, and bottom. The coal from the king seam of 6.5 m thick is exploited with continuous miner technology; however, the bord and pillar methods are adopted for the bottom and top seams. In the continuous miner method, the developed galleries are heightened to 4.6 m and widened to 6.5 m to commence depillaring operation. The pillar is divided into fenders and commences the extraction of coal in the slices (3.3 m) leaving ribs (3.0 m) between two consecutive slices. The panel and extraction sequence of the pillar in the study panel is shown in Figure 4.

Figure 4 Continuous miner workings of panel 11-A3, (a) the panel no. 11-A3 (b) cutting sequence (see online version for colours)

(a)

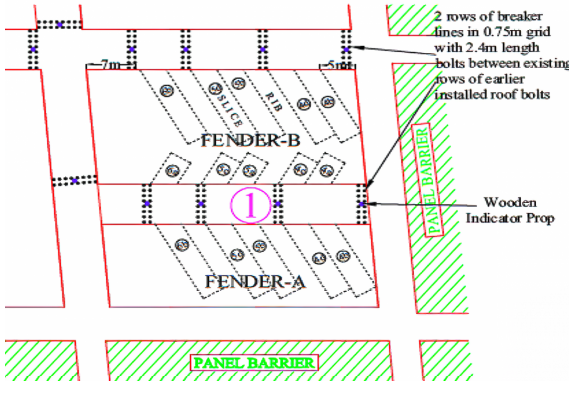

(b)

As mentioned in Table 1, the study panel consists of 13 pillars with an average size of 45 m × 43 m. The total area and average depth of the panel are 28,300 sq.m and 305 m respectively. For the development of CMWI, the convergence data of the other two panels 11A-2 and 11A-3 are also collected. Table 1 lists details of the three panels namely, 11A-1, 11A-2, and 11A-3.

Table 1 Details of the panels 11A-1, 11A-2 and 11A-3

Parameters	*Panel 11A-1*	*Panel 11A-2*	*Panel 11A-3*
Panel length (m)	180.00	145.00	200.00
Panel width (m)	145.00	140.00	141.00
Number of pillars	14	9	13
Area of the panel (sq.m)	30,500	20,300	28,300
Average pillar size (m)	42 m × 40 m	45 m × 43 m	45 m × 43 m
Height of extraction (m)	4.6	4.6	4.6
Panel depth (m)	317.00	313.00	315.00
Length of split (m)	38.0	38.0	38.0
Width of split (m)	6.5	6.5	6.5
Maximum cut off distance in split (m)	15	15	15
Maximum cut off distance in slice (m)	14	14	14
Length of a rib (m)	14.0	14.0	14.0
Thickness of a rib (m)	3.0	3.0	3.0
Size of a stook (m)	7 m × 13.5 m	7 m × 13.5 m	7 m × 13.5 m

Figure 5 Mine plan of the panel 11A-1 (see online version for colours)

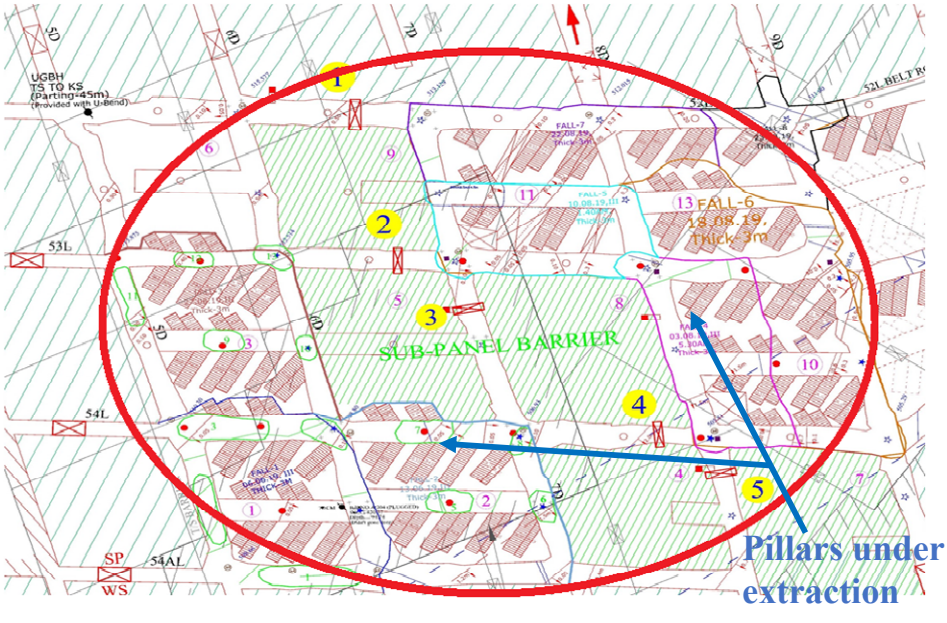

Figures 5 and 6 show the plans of 11A-1 and 11A-2 panels situated at an average depth of 315 m and 310 m respectively. Figure 7 shows the lithology of the mine site.

Figure 6 Mine plan of the panel 11A-2 (see online version for colours)

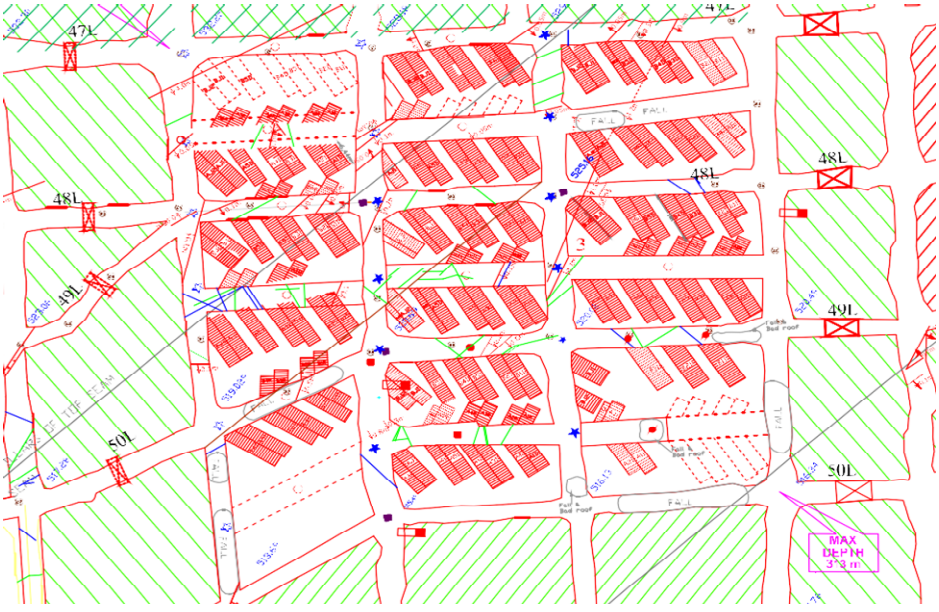

Figure 7 The lithology of a mine site (see online version for colours)

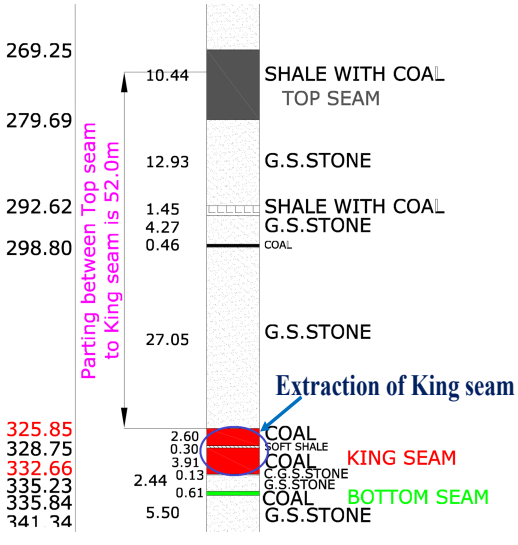

Table 2 lists the material properties such as compressive strength, tensile strength, rock mass rating (RMR), modulus of elasticity, cohesion, and angle of internal friction of the continuous miner panels 11A-1, 11A-2 and 11A-3 of the mines.

In this study, each panel is sectionalised into three zones based on the condition of the roof or RMR of the immediate roof, such as weak (M1), moderate week (M2), and strong (M3). The average RMR of the panels are estimated based on five parameters: strength of the rock, rock quality designation, condition of discontinuities, the spacing of discontinuities, and groundwater and RMR values of three zones which are estimated to be 45, 50 and 60 respectively. The RMR values are used for the derivation of the CMWI to estimate the RC in the panel as mentioned in Section 4.

Table 2 Material properties of the panels

Panels		*Compressive strength, σ_c (MPa)*	*Tensile strength, σ_t (MPa)*	*RMR*	*Modulus of elasticity (GPa)*	*Cohesion (MPa)*	*Internal friction angle (degree)*
Panel 11A-1	M1	4.22	0.52	45	1.6	1.42	27
	M2	4.31	0.57	50			
	M3	4.52	0.59	55			
Panel 11A-2	M1	4.12	0.51	45	1.58	1.42	27
	M2	4.29	0.54	50			
	M3	4.61	0.59	55			
Panel 11A-3	M1	4.19	0.499	45	1.56	1.42	27
	M2	4.38	0.53	50			
	M3	4.49	0.49	55			

3.2 Measurement of RC with the developed system

The developed system is deployed in the split and main roadways of working panel 11A-3 at various locations (5 m, 10 m, 15 m, 20 m, and 25 m) from the face and record the development of RC based on the retreat distance of the workings. Figure 8 shows the deployment of the system at the mine. The developed RC is measured continuously and is sent to the receiver through the transmitter. It is observed that the RC increases with an increase of the retreat distance within the periodic weighting zone. After the fall occurs in the goaf, the convergence value reduces and increases with the retreat distance. Figure 9 show the development of RC at 5 m, 10 m, 15 m, 20 m, and 25 m stations. It is observed from the figures that the convergence values are measured at a 1 mm interval since the system measures a minimum convergence of 1 mm.

Roof monitoring devices such as tell-tale, stress cells, and load cells are installed to monitor the roof dilations and load. The convergence data of tell-tale is compared with that of the developed system to investigate the accuracy of results. Figure 9 shows the comparison of the convergence readings of the new system and the tell-tale.

It is also observed from Figure 9 that the RC increases with an increase in retreat distance in both cases. However, the convergence values obtained by the developed system follow almost a straight line.

Figure 8 Deployment of a developed system (see online version for colours)

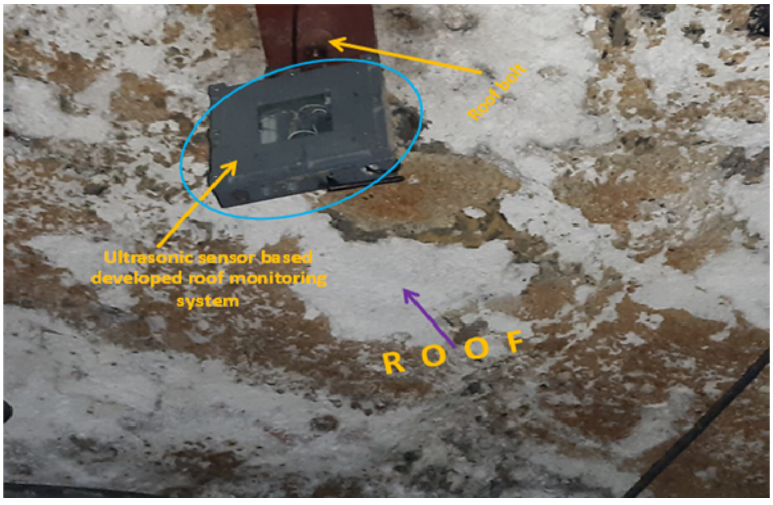

Figure 9 Comparison of the convergence readings (see online version for colours)

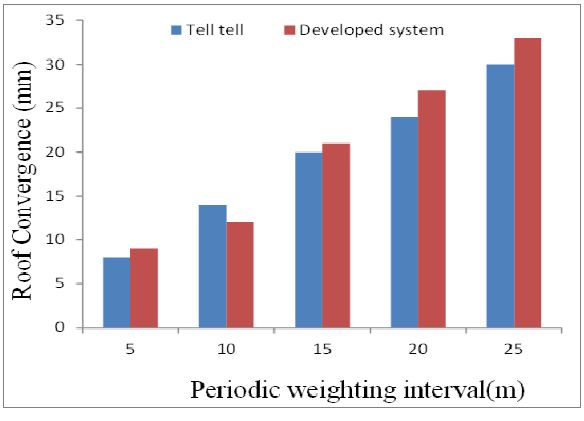

4 Analysis of RC developed in continuous miner workings

In this section, RC data generated due to retreating of the face is analysed to derive CMWI. Using the working index, RC may be estimated for any similar existing mining condition of the mine site. As mentioned before, the RC values of three panels' 11A-1, 11A-2, and 11A-3 measured by tell-tale are collected for development of CMWI. The RC at five locations (retreat distance of 5 m, 10 m, 15 m, 20 m, and 25 m) in three different zones of the panel is recorded. Figure 10 and Figure 11 are plotted to represent the typical variation of RC with a ratio of retreat distance to that of maximum retreat length (R / RMR_{max}) and RMR of the immediate roof to that of a maximum value of working panels (RMR / RMR_{max}) respectively for all combinations of mining depth.

Figure 10 Behaviour of RC of continuous miner workings with different immediate roof material (see online version for colours)

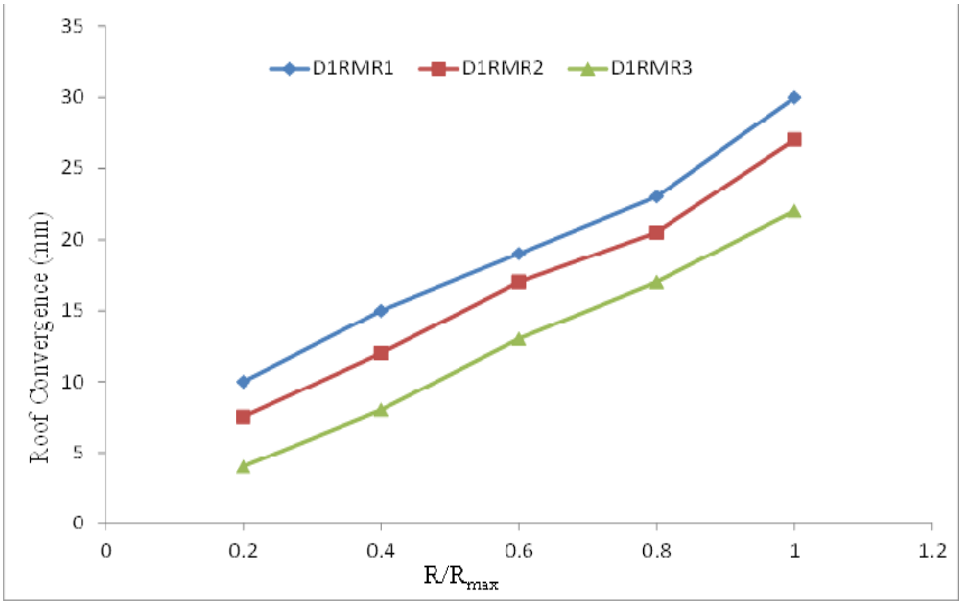

Figure 11 Behaviour of RC of continuous miner workings with different retreat distance (see online version for colours)

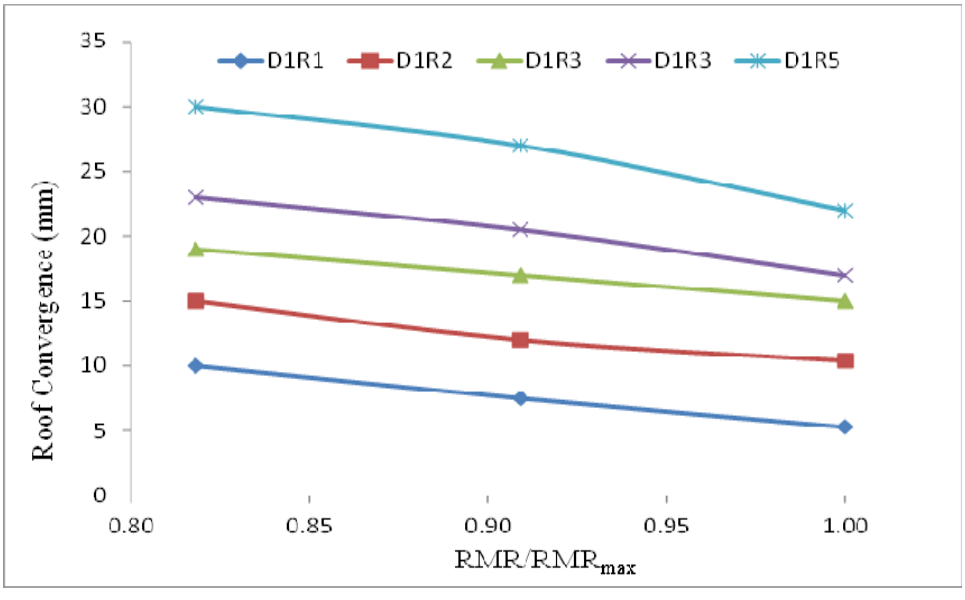

From Figure10, it is found that RC in continuous miner workings increases with the improvement of R_k/R_{max} quantity, where R is the retreat distance. It is also observed that higher RC in weak material (M1) or low RMR and lesser in panel (M3) or high RMR of CM workings. As expected from Figure 11, the maximum RC in the CM workings is

found to be maximum in the D1R5 curve and minimum in the D1R1 curve for a given RMR of the panel.

4.1 Development of mine index

It is observed from the curves (Figures 10 and 11) that RC in the continuous miner workings is proportional to R_k/R_{max} and inversely proportional to RMR_j/RMR_{max}. So, a mine roof index is defined based on the retreat distance and RMR of mine roof, as mentioned in equation (1).

$$MI = \frac{R_k / R_{\max}}{RMR_j / RMR_{\max}} \tag{1}$$

The basic idea of developing the mine index (MI) is to merge retreat distance and RMR of the panel or material variability into a single parameter and to develop a linear variation of RC with MI. As given above, it is understood that RC changes linearly with MI as mentioned in equation (2),

$$RC = \alpha(MI) + \beta \tag{2}$$

Now, considering $x_1 = R_k/R_{max}$, $x_2 = RMR_j/RMR_{max}$ and $z = RC - \beta$ and applying natural logarithm to equation (1), we find

$$\ln z = \ln \alpha + \ln(x_1) - \ln(x_2) \tag{3}$$

In the above equation, there are two unknowns viz. α, β. The least-square error can be expressed as follows:

$$RC = \frac{1}{2}\sum_{k=1}^{N}\left[\ln(z_k) - \ln(\hat{z}_k)\right]^2 \tag{4}$$

where N is the number of samples for a particular mining depth (D_p). Considering minimisation error, α and β values are obtained for main roof thickness D_p = 325 m, 340 m and 355 m.

Table 3 Slopes (α) and intercepts (β) of the linear relationship between *MI* and RC

D_p	α	β
D1 =325 m	23.141	7.324
D2 = 340 m	24.134	9.5645
D3 =355 m	24.58	12.201

From the above analysis, MI can be determined [equation (1)] for a given depth of the panel D_p. A detailed methodology is established to merge panel depth with MI to form a combined index known as 'CMWI', which can be used to estimate *RC* that may occur in continuous miner workings. Once the CMWI is determined, RC in CM workings can also be estimated for a similar mine working condition. And also, mine operators may take appropriate decisions to move coal face or withdrawing machine from working face. Mathematically, RC depended on *MI* and D_p as mentioned in equation (5).

$$RC = f(MI, D_p) \tag{5}$$

4.2 Merging MI and D_p

There are 15 variations of MI, three variations of RMR and five variations for retreat distance of CM workings. From 45 observations, three groups were formed by combining 15 observations with retreat distance and RMR of immediate roof for a given D_p. The, three lines have been drawn using equation (1) for depth of the panel (D_p) and shown in Figure 12.

Figure 12 RC versus MI for different main roof lengths (see online version for colours)

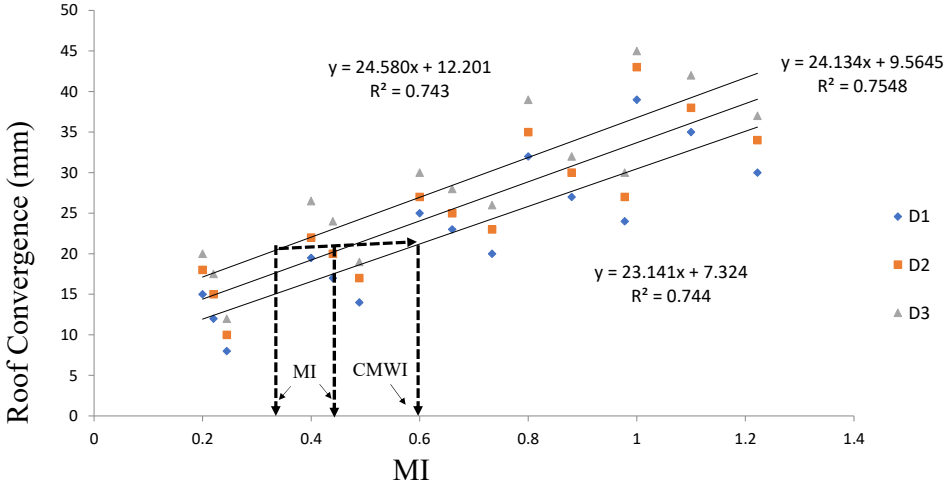

Considering, m = 1, 2 and 3 for mining depth of D = 325 m, 340 m, and 355 m respectively, equation (1) can be formulated as,

$$RC_m = (MI)\alpha_m + \beta_m \tag{6}$$

The major idea is to transfer data points of RC_{D2} and RC_{D3} lines onto line RC_{D1} by changing the abscissa (or *RI* value) of each data point (of lines RC_{D2} and RC_{D3}) such that *RC* values remain constant as shown by dotted lines in Figure 12. Thus, a new abscissa (*CMWI*) for each point in lines representing RC_{D2} and RC_{D3} is found by simply re-plotting ordinates of RC_{D2} and RC_{D3} into the equation of RC_{D1} as given below.

$$\beta_1 + (CMWI)\alpha_1 - RC_m = 0, \quad \text{where } m = 2 \text{ and } 3 \tag{7}$$

Equation (7) is solved for obtaining solution of CMWI for RC_{D2} and RC_{D3}. It is clear that CMWI for RC_{D1} (for $D1$ = 325 m) remains the same as the data points on this line are unaltered. A composite line for RC_{D2} and RC_{D3} in Figure 12, shows the combined effect of *MI* and panel depth (D_p). This shows that each of the three lines in Figure 12 is combined into one (Figure 13). It may be noted that abscissa of Figure 12 is now *CMWI* instead of *MI* as given in Figure 13. The relationship between *RC* and *MI* is as follows.

$$RC = 23.14(CMWI) + 7.323 \tag{8}$$

Figure 13 RC vs. CMWI (see online version for colours)

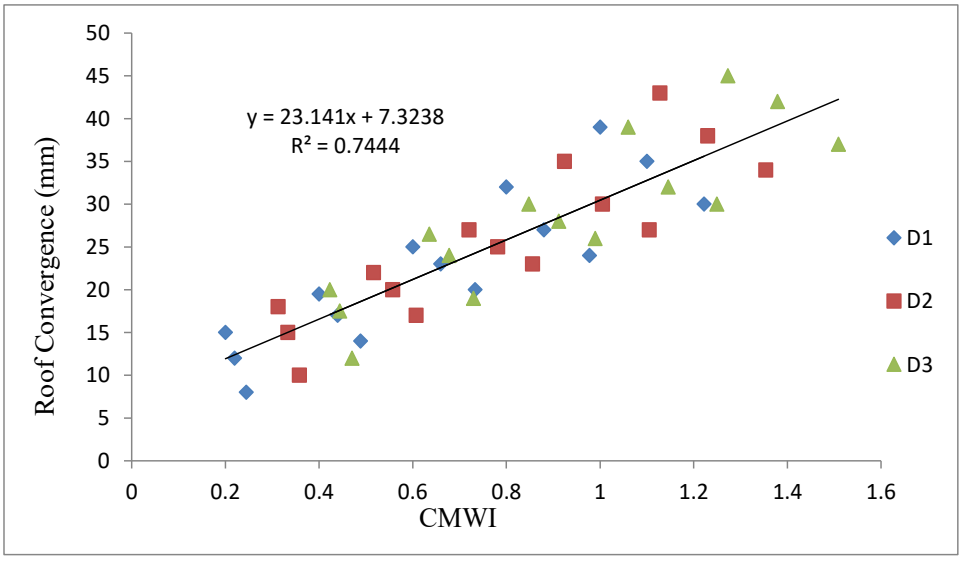

Table 4 Slopes (ζ) and intercepts (η) of the linear relationship between *MI* and *CMWI*

D_p	ζ	η
D1 = 325 m	1	0
D2 = 340 m	1.0185	0.1092
D3 = 355 m	1.0622	0.2108

Figure 14 Relation between CMWI and MI for different main roof lengths (see online version for colours)

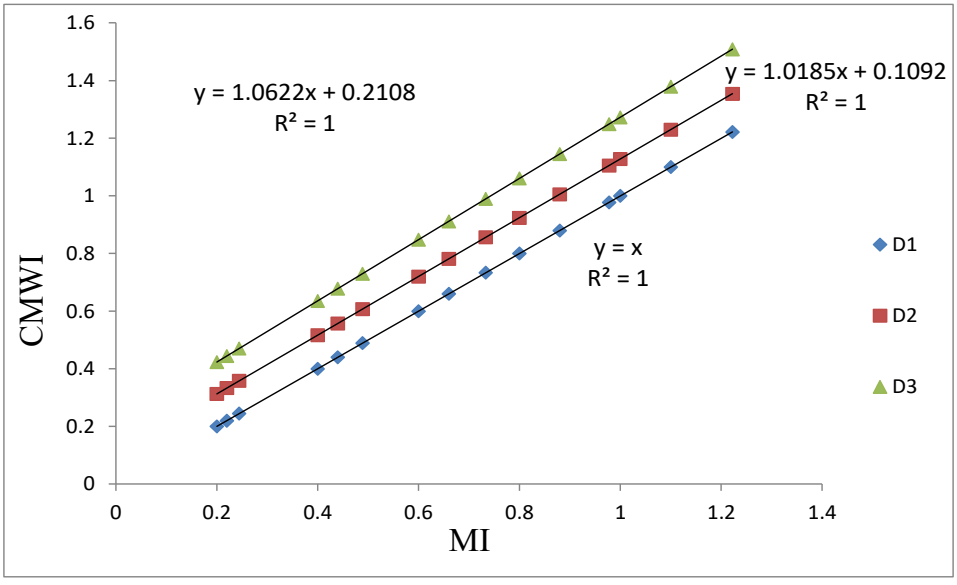

Now, the linear relationship (Figure 14) between indices *MI* and *CMWI* can be generated to obtain the effect of *MI* on *RC* for mining depths of 325 m,340 m, and 355 m respectively. The general form of the relationship between MI and CMWI is given below.

$$CMWI = \zeta_m MI + \eta_m \tag{9}$$

From the analysis carried above, the combined composite index *CMWI* can be given as

$$CMWI = \eta_m + \zeta_m \left(\frac{R/R_{\max}}{RMR/RMR_{\max}} \right), \quad \text{where } m = 1, 2, \text{ and } 3 \tag{10}$$

The slope and intercepts of the above equations are shown in Tables 3 and 4. The above index is valid statistically for given boundary conditions of geo-mining condition of the CM workings (Verma and Deb, 2010; Islavath et al., 2020).

5 Conclusions

This study proposes an innovative system that was developed based on the ultrasonic sensor for monitoring RC in underground workings and this system measures and transmits the signals to the receiver. The convergence data of this system is compared with that of tell-tale measured data and was found to be satisfactory. The RC data is further processed using the statistical method and a composite index called CMWI was developed by incorporating all the input variables such as retreat distance, RMR, and mining depth. This index can be useful to predict the convergence in continuous miner workings and accordingly, the mine management may decide for the withdrawal of men and machinery deployed in the workings if any unwanted convergence is found.

References

Atul, K., Dheeraj, K., Singh, U.K. and Gupta, P.S. (2010) 'Development of an automated system for continuous monitoring of powered roof support in longwall panel', *Journal of Coal Science and Engineering (China)*, Vol. 16, No. 4, pp.337–340, https://doi.org/10.1007/s12404-010-0401-3.

Buddery, P., Morton, C., Scott, D. and Owen, N. (2018) 'A continuous roof and floor monitoring systems for tailgate roadways', in *Proceedings of the 18th coal operators' conference*, University of Wollongong, pp.72–81.

DGMS (2017) *Standard Note*, Directorate General of Mines Safety, India [online] http://dgms.gov.in/writereaddata/UploadFile/Standard_Note_01-01-20176362197732330444487.pdf (accessed 12 January 2018).

Gong, H., Kizil, M.S., Chen, Z., Amanzadeh, M., Yang, B. and Aminossadati, S.M. (2019) 'Advances in fibre optic based geotechnical monitoring systems for underground excavations', *International Journal of Mining Science and Technology*, Vol. 29, No. 2, pp.229–238, https://doi.org/10.1016/j.ijmst.2018.06.007.

Indra, S.K., Padhee, S. and Pati, U.C. (2018) 'Design of wireless electronic telltale system for indication of rock deformation', *IEEE Sensors Letters*, Vol. 2, No. 3, pp.1–4, https://doi.org/10.1109/LSENS.2018.2845708.

Islavath, S.R., Deb, D. and Kumar, H. (2020) 'Development of a roof-to-floor convergence index for longwall face using combined finite element modelling and statistical approach', *International Journal of Rock Mechanics and Mining Sciences*, Vol. 127, Nos. 1–11, p.104221, https://doi.org/10.1016/j.ijrmms.2020.104221.

Jena, S.K., Lokhande, R.D., Pradhan, M. and Kumar, N. (2019) 'Development of a model to estimate strata behaviour during bord and pillar extraction in underground coal mining', *Arabian Journal of Geosciences*, Vol. 12, No. 7, p.242, https://doi.org/10.1007/s12517-019-4381-5.

Katkuri, S., Deb, D., Reddy, B.V. and Kumar, H. (2019) 'Neural network assisted analysis for longwall gate road stability using measured roof convergence data', *Geotechnical and Geological Engineering*, Vol. 37, No. 5, pp.3843–3860, https://doi.org/10.1007/s10706-019-00873-6.

Kumarghosh, S., Bhattacharjee, S., Rao, K., Ded, D. and Pal, S. (2011) 'Underground coal mine instrumentation using electromagnetic sensors for roof health monitoring and fall prediction', *International Journal of Earth Sciences and Engineering*, Vol. 4, No. 2, pp.328–335.

MSHA (2017) *Preliminary Accident Reports, Fatality Alerts, and Fatal Accident Reports*, Mines Safety and Health Administration, USA [online] https://arlweb.msha.gov/fatals/ (accessed 26 March 2018).

Nicolau, V., Miholca, C. and Andrei, M. (2009) 'Fuzzy rules of sound speed influence on ultrasonic sensing in outdoor environments', *3rd International Workshop on Soft Computing Applications*, IEEE, July, pp.145–150, https://doi.org/10.1109/SOFA.2009.5254862.

Panda, K.G., Agrawal, D., Nshimiyimana, A. and Hossain, A. (2016) 'Effects of environment on accuracy of ultrasonic sensor operates in millimetre range', *Perspectives in Science*, Vol. 8, No. 9, pp.574–576, https://doi.org/10.1016/j.pisc.2016.06.024.

Shen, B.K.A.G.H., King, A. and Guo, H. (2008) 'Displacement, stress and seismicity in roadway roofs during mining-induced failure', *International Journal of Rock Mechanics and Mining Sciences*, Vol. 45, No. 5, pp.672–688, https://doi.org/10.1016/j.ijrmms.2007.08.011.

Swanson, P. (2002) 'Feasibility of using laser-based vibration measurements to detect roof fall hazards in underground mines', *Fifth International Conference on Vibration Measurements by Laser Techniques: Advances and Applications*, International Society for Optics and Photonics, May Vol. 4827, pp.541–552, https://doi.org/10.1117/12.468158.

Verma, A.K. and Deb, D. (2010) 'Longwall face stability index for estimation of chock-shield pressure and face convergence', *Geotechnical and Geological Engineering*, Vol. 28, No. 4, pp.431–445, https://doi.org/10.1007/s10706-010-9303-y.

Zhang, K., Ji, S., Zhang, Y., Zhang, J. and Pan, R. (2018) 'MEMS inertial sensor for strata stability monitoring in underground mining: an experimental study', *Shock and Vibration*, Vol. 2018, No. 6, p.8, https://doi.org/10.1155/2018/4895862.

Zhao, Z.G., Zhang, Y.J., Li, C., Wan, Z., Li, Y.N., Wang, K. and Xu, J. F. (2015) 'Monitoring of coal mine roadway roof separation based on fiber Bragg grating displacement sensors', *International Journal of Rock Mechanics and Mining Sciences*, Vol. 74, pp.128–132, http://dx.doi.org/10.1016%2Fj.ijrmms.2015.01.002.